The EMBO Journal Vol. 20 No. 14 pp. 3695–3704, 2001

A nuclear AAA-type ATPase (Rix7p) is required for biogenesis and nuclear export of 60S ribosomal subunits

Olivier Gadal, Daniela Strauß, Joris Braspenning, Dominic Hoepfner[1], Elisabeth Petfalski[2], Peter Philippsen[1], David Tollervey[2] and Ed Hurt[3]

BZH, Biochemie-Zentrum Heidelberg, Im Neuenheimer Feld 328, D-69120 Heidelberg, Germany, [1]Biozentrum der Universität Basel, Klingelbergstraße 70, CH-4056 Basel, Switzerland and [2]Institute of Cell and Molecular Biology, University of Edinburgh, Swann Building, King's Buildings, Edinburgh EH9 3JR, UK

[3]Corresponding author
e-mail: cg5@ix.urz.uni-heidelberg.de

Ribosomal precursor particles are assembled in the nucleolus before export into the cytoplasm. Using a visual assay for nuclear accumulation of 60S subunits, we have isolated several conditional-lethal strains with defects in ribosomal export (*rix* mutants). Here we report the characterization of a mutation in an essential gene, *RIX7*, which encodes a novel member of the AAA ATPase superfamily. The *rix7-1* temperature-sensitive allele carries a point mutation that causes defects in pre-rRNA processing, biogenesis of 60S ribosomal subunits, and their subsequent export into the cytoplasm. Rix7p, which associates with 60S ribosomal precursor particles, localizes throughout the nucleus in exponentially growing cells, but concentrates in the nucleolus in stationary phase cells. When cells resume growth upon shift to fresh medium, Rix7p–green fluorescent protein exhibits a transient perinuclear location. We propose that a nuclear AAA ATPase is required for restructuring nucleoplasmic 60S pre-ribosomal particles to make them competent for nuclear export.

Keywords: AAA ATPase/nuclear transport/ribosomal biogenesis/ribosomal export

Introduction

The nucleolus is a specialized subnuclear compartment in which most steps of ribosome biogenesis take place. This process starts with the synthesis of two pre-rRNA transcripts, pre-5S rRNA and a large RNA polymerase I transcript (35S pre-rRNA in yeast), which is processed to the mature 25S/28S, 18S and 5.8S rRNAs (Kressler *et al*., 1999). The 5S RNA is transcribed by RNA polymerase III and recruited separately to the assembling ribosome (Dechampesme *et al*., 1999). Ribosomal proteins are synthesized in the cytoplasm and imported into the nucleus, where they associate with newly transcribed pre-rRNAs to generate pre-ribosomal particles (Woolford, 1991). In contrast to pre-rRNA processing and modification, very little is known about the assembly pathway for eukaryotic ribosomal subunits (Venema and Tollervey, 1999). However, it is clear that the assembly of pre-ribosomes is closely coordinated with rRNA maturation and transport. A succession of steps leads to the formation of particles competent for release from the nucleolus and export from the nucleus (for a recent review see Kressler *et al*., 1999).

The mechanism of ribosome biogenesis appears to be well conserved throughout eukaryotes. Many components involved in this complex process were identified and characterized in *Saccharomyces cerevisiae*, where >60 *trans*-acting factors are required to synthesize the mature 60S and 40S subunits. These include rRNA-modifying enzymes, endonucleases, exonucleases, RNA helicases and proteins associated with the small nucleolar RNAs (snoRNAs) (Kressler *et al*., 1999). The majority of these factors are enriched in the nucleolus. However, some are detected in the cytoplasm (Kressler *et al*., 1999) or associated with the nuclear pore complex (NPC) (Rout *et al*., 2000).

Saccharomyces cerevisiae has proven to be useful for the analysis of the NPC and the nuclear export of proteins, tRNA or mRNA (Amberg *et al*., 1992; Kadowaki *et al*., 1992; Doye and Hurt, 1997; Segref *et al*., 1997; Stade *et al*., 1997; Hellmuth *et al*., 1998; Sarkar *et al*., 1999). The analysis of nuclear export of ribosomes has been aided by the development of functional green fluorescent protein (GFP)-tagged ribosomal protein reporters. We have previously reported an *in vivo* export assay that uses the large subunit reporter Rpl25p–eGFP (Hurt *et al*., 1999; Gadal *et al*., 2001). Rpl25p is imported into the nucleus and assembles with ribosomes by direct binding to the rRNA inside the nucleolus (Van Beekvelt *et al*., 2000). This assay showed that a subset of nucleoporins and the Ran system are required for nuclear 60S subunit export. Analysis using a different ribosomal protein–GFP fusion gave similar results (Stage-Zimmermann *et al*., 2000). We have exploited the Rpl25p–eGFP assay to identify new factors required for nuclear 60S subunit export (Gadal *et al*., 2001; Milkereit *et al*., 2001).

Here we report the characterization of the *rix7-1* mutant, which is complemented by YLL034c encoding a previously uncharacterized member of the AAA family of ATPases. AAA proteins act in a variety of cellular functions, including cell cycle regulation, protein degradation, organelle biogenesis and vesicular transport; hence, the origin of their name 'ATPases associated with different activities'. The AAA domain is highly conserved among this family and a common mechanism of action has been proposed. A nucleotide-dependent conformational switch is proposed to apply tension to bound proteins, allowing AAA proteins to unfold polypeptides, dissociate protein–protein interactions or generate unidirectional movement (Rouiller *et al*., 2000; Vale, 2000). We show that Rix7p is

located in the nucleus, and is required for 60S biogenesis and subsequent nuclear export.

Results

Isolation of the rix7-1 mutant, which is impaired in the export of ribosomes from the nucleolus to the cytoplasm

The screen for nuclear accumulation of the large subunit reporter Rpl25p–eGFP (Gadal *et al.*, 2001) identified *rix7-1*, which shows slow growth at permissive temperatures (doubling times of 2.8 h for *rix7-1* strains at 23°C and of 2 h for the wild-type strain) and ceases growth 5 h after shift to the restrictive temperature of 37°C (Figure 1A). At 23°C, Rpl25p–eGFP was cytoplasmic with nuclear exclusion in the *rix7-1* strain, but strong nuclear accumulation was observed 2–3 h after transfer to 37°C (Figure 1B). The *rix* phenotype was, therefore, visible before a distinct growth defect was observed at 37°C. The pattern of accumulation of Rpl25p–eGFP inside the nucleus was found to be different in the various *rix* mutants (Gadal *et al.*, 2001). In some *rix* mutants, Rpl25p–eGFP accumulates throughout the nucleoplasm, whereas in other mutants, including *rix7-1*, Rpl25p–eGFP accumulates predominantly in the nucleolus (Figure 1B, insert). This suggests that following transfer of the *rix7-1* cells to 37°C, release of pre-ribosomal particles from the nucleolus to the nucleoplasm is inhibited.

The wild-type *RIX7* gene was cloned by complementation of the *rix7-1* temperature-sensitive (ts) phenotype, and corresponds to locus *YLL034c*, which encodes an essential and novel protein of 92 kDa (see below). Cloned *YLL034c* complemented the growth defect of *rix7-1* (Figure 2A) and rescued the nuclear accumulation of Rpl25p–eGFP. However, a few percent of the complemented cells still exhibited nuclear accumulation of Rpl25p–eGFP (data not shown). Similarly, the pre-rRNA processing defect was not completely rescued by expression of *YLL034c* (see below), indicating that the *rix7-1* mutation is semi-dominant. To show that the *rix7-1* mutation lies in the *YLL034c* gene locus and to isolate the mutant allele, DNA from the chromosomal locus was recovered by PCR from *rix7-1* and isogenic wild-type strains. A single nucleotide substitution was found in the *YLL034c* open reading frame of *rix7-1*, changing proline (224) to leucine. The recovered *rix7* allele was inserted into an *ARS/CEN* plasmid. When expressed in a *rix7*-Δ strain, the cloned allele conferred ts growth and nuclear accumulation of Rpl25p–eGFP similar to the original *rix7-1* strain. Mild nuclear accumulation of Rpl25p–eGFP was also observed when the recovered *rix7* allele was expressed in a wild-type strain (data not shown), consistent with the semi-dominant phenotype of *rix7-1*. We conclude that the Pro_{224}→Leu mutation in *YLL034c* is responsible for the *rix7-1* phenotype.

Next, we wanted to know whether the *RIX7* gene is functionally linked to other components involved in ribosomal export. Mutations in the ribosomal protein Rpl10p, a late nuclear assembling component of 60S ribosomal subunits, can give rise to a *rix* phenotype (Gadal *et al.*, 2001). Rpl10p acts, at least in part, by recruiting Nmd3p to the 60S ribosomal subunit. Nmd3p, in turn, is an adapter for the exportin Xpo1p, which exports NES-containing proteins from the nucleus to the cytoplasm (Ho *et al.*, 2000; Gadal *et al.*, 2001). As shown in Figure 2B, the *rix7-1* mutation is synthetically lethal with the *rpl10-2* allele, indicating that Rix7p and Rpl10p also functionally interact.

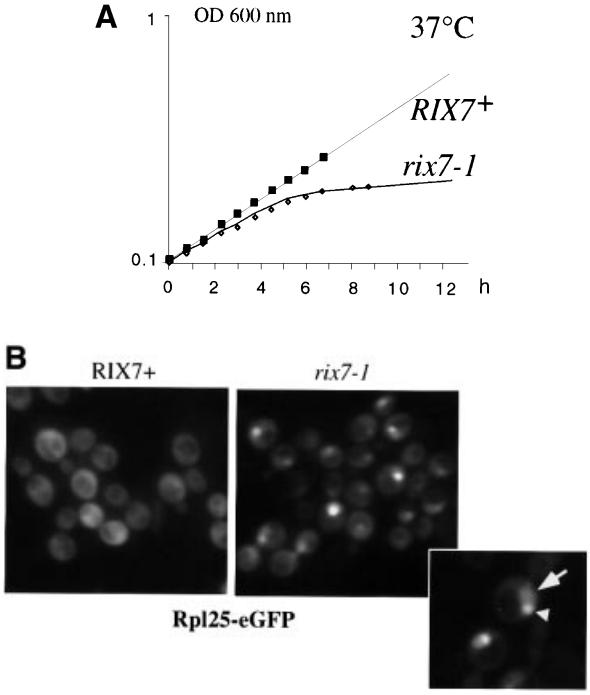

Fig. 1. Nuclear accumulation of Rpl25p–eGFP in *rix7-1* cells. (**A**) Growth curve of *rix7-1* and isogenic wild-type cells at 37°C. (**B**) *rix7-1* and isogenic wild-type cells expressing Rpl25p–eGFP were grown at 23°C, before shift for 5 h to 35°C and inspection in the fluorescence microscope. The arrowhead points to nuclear staining and the triangle to nucleolar staining.

Rix7p is a conserved nuclear member of the AAA ATPase family

A search for conserved motifs in Rix7p revealed the presence of two AAA ATPase domains (residues 241–430 and 569–737; Neuwald *et al.*, 1999) and a putative bipartite nuclear localization signal (NLS) in the N-terminal region (residues 175–195; Figure 3A, upper panel). To identify functionally important regions within Rix7p, a set of N- and C-terminal deletions was generated. A construct deleted of the N-terminal amino acids 1–174 (ΔN) was functional, whereas a longer N-terminal deletion of 1–202, including the putative NLS (ΔN+NLS), no longer supported growth (Figure 3A). A short C-terminal deletion of 776–837 (ΔC) also leads to loss of function (Figure 3A). The short C-terminal region of Rix7p that lies outside of the AAA domains is, therefore, essential for cell growth.

Fluorescence microscopy revealed that full-length Rix7p–GFP is nuclear in exponentially growing cells (Figure 3B). The functional Rix7pΔN–GFP shows a similar localization, but removal of the putative NLS (ΔN+NLS) causes a cytoplasmic location (Figure 3B). Furthermore, the corresponding (N+NLS)–GFP construct is nuclear (Figure 3B). Thus, Rix7p contains a single functional NLS in its N-terminal region (Figure 3A).

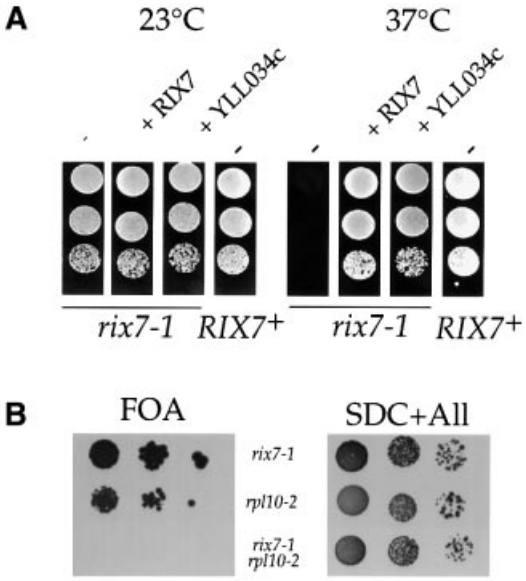

Fig. 2. *rix7-1* is complemented by *YLL034c*, which is genetically linked to *RPL10*. (**A**) *rix7-1* is complemented by *YLL034c*. Growth of wild-type yeast (*RIX7*$^+$) and the *rix7-1* ts strain harbouring an empty plasmid (-), a plasmid with a 10 kb genomic insert containing YLL034c (pRIX7) or a plasmid containing only *YLL034c*. YPD plates were incubated for 4 days at 23 or 37°C. (**B**) Synthetic lethal relationship between *rix7-1* and *rpl10-2*. Synthetic lethality was analysed by the ability to lose wild-type *RPL10* present on a *URA3*-containing plasmid in the haploid double mutant *rix7-1/rpl10-2* (see Table I). For comparison, the growth of haploid single mutants *rix7-1*and *rpl10-2* is shown. Growth was analysed after 4 days at 23°C on 5-fluoroorotic acid (FOA)-containing plates (left panel) or SDC+All (minimal glucose medium plus all nutrients) plates.

However, a construct with the short C-terminal deletion (ΔC), although still nuclear, is not functional, demonstrating that this part of Rix7p plays a different essential role.

Rix7p shows high homology to all members of the AAA ATPase superfamily (data not shown). However, human NVL (Germain-Lee *et al*., 1997) and *Schizosaccharomyces pombe* SPBC16E9.10c may be the orthologues of Rix7p since additional conserved motifs can be identified in these two proteins, including the essential C-terminal domain, in addition to the two AAA domains (Figure 3C). No clear homology was detected within the non-essential N-terminal domain of Rix7p, but a putative NLS is present just before the first AAA domain of the human and *S.pombe* counterparts (data not shown).

Rix7p is involved in 60S ribosomal subunit biogenesis

The nucleolar/nuclear accumulation of Rpl25p–eGFP observed in the *rix7-1* ts mutant (see Figure 1B) and the localization of Rix7p (see Figure 3B) suggest a role of Rix7p in the biogenesis of large ribosomal subunits. Defects in 60S subunit biogenesis generally result in decreased free 60S subunits and the appearance of 'half-mer' polysomes (polysomes containing an unjoined 40S subunit at the initiation site). The sucrose density gradient profile of polysomes isolated from *rix7-1* cells grown at the permissive temperature was similar to that of the isogenic wild type (Figure 4A). Following transfer of the *rix7-1* strain to 37°C, the free 60S subunit peak was reduced, while the 40S peak increased (Figure 3A). The polysomal peaks were also reduced and half-mers were readily detected.

To observe the decrease in 60S ribosomal subunits in *rix7-1* cells more directly, 40S and 60S subunits were dissociated with high salt (0.8 M KCl) before sucrose density gradient centrifugation (Figure 4B). The 60S:40S ratio measured by UV absorption is ~2 in wild-type strains, but decreased to 0.85 in the *rix7-1* strain after shift to 37°C (Figure 4B). This strong depletion of 60S subunits suggests that Rix7p functions in large subunit biogenesis.

Pre-rRNA processing is defective in rix7-1 mutant strains

To test whether the depletion of 60S ribosomal subunits observed in the *rix7-1* strain is a consequence of defects in pre-rRNA processing, this was analysed by northern hybridization (Figure 5B and C), primer extension (Figure 5D) and pulse–chase analysis (Figure 6). Following transfer of the *rix7-1* strain to 37°C for 2 h, the precursors on the pathway of 25S and 5.8S rRNA synthesis, the 27SB, 7S and 6S pre-rRNAs, are very strongly reduced (Figure 5). By 4 h after transfer to 37°C, the mature 5.8S and 25S rRNAs are seen to be depleted, consistent with the reduced amount of 60S subunit in the *rix7-1* strain at 37°C. In addition, the 35S pre-rRNA was accumulated, accompanied by some reduction in the levels of the 27SA$_2$ and 20S pre-rRNAs. A low level of the 23S pre-rRNA, which is generated from the 35S by cleavage at site A$_3$ in the absence of prior cleavage at sites A$_0$, A$_1$ and A$_2$, was also detected. These phenotypes reveal a delay in the three early cleavages at sites A$_0$, A$_1$ and A$_2$ in the *rix7-1* strain.

Primer extension analysis indicated that cleavage at sites A$_2$ (Figure 5D), A$_0$ and A$_3$ (data not shown) continued. Primer extension stops at sites B1$_L$ and B1$_S$ were detected at low levels, but with no clear change in their relative efficiencies (Figure 5D). All cleavages were accurate at the nucleotide level. We conclude that processing of the pre-rRNA at sites A$_3$, B1$_L$ and B1$_S$ continues in the *rix7-1* strain, followed by rapid degradation of the 27SB pre-rRNAs. In wild-type cells, a low level of a pre-rRNA that extends from site A$_2$ to site E (the 3′ end of the 5.8S rRNA) is observed (Figure 5C). In the *rix7-1* mutant, this is lost and replaced by a species that extends from A$_2$ to C$_2$ (the 3′ end of the 7S pre-rRNA). We conclude that some pre-rRNA cleavage at site C$_2$ also continues in the mutant strains. Together with the continued processing at B$_1$, this indicates that some level of the 7S pre-rRNA continues to be synthesized and rapidly degraded. Notably, no intermediates on the pathway of 25S/5.8S synthesis were accumulated in the *rix7-1* strains, making it unlikely that loss of the mature rRNAs is primarily due to a defect in pre-rRNA cleavage.

Pulse–chase labelling of the *rix7-1* strain 2 h after transfer to 37°C, with either [^{3}H]uracil or [^{3}H]methyl methionine, showed a dramatic reduction in the synthesis of both the 25S and 5.8S rRNAs (Figure 6). The 35S pre-rRNA was synthesized and showed some retardation in its processing. The 27SA pre-rRNA was also synthesized with some delay in the *rix7-1* strain, but the 27SB and 7S pre-rRNAs were not detected. Synthesis of the 20S pre-rRNA and 18S rRNA continued, with a delay consistent

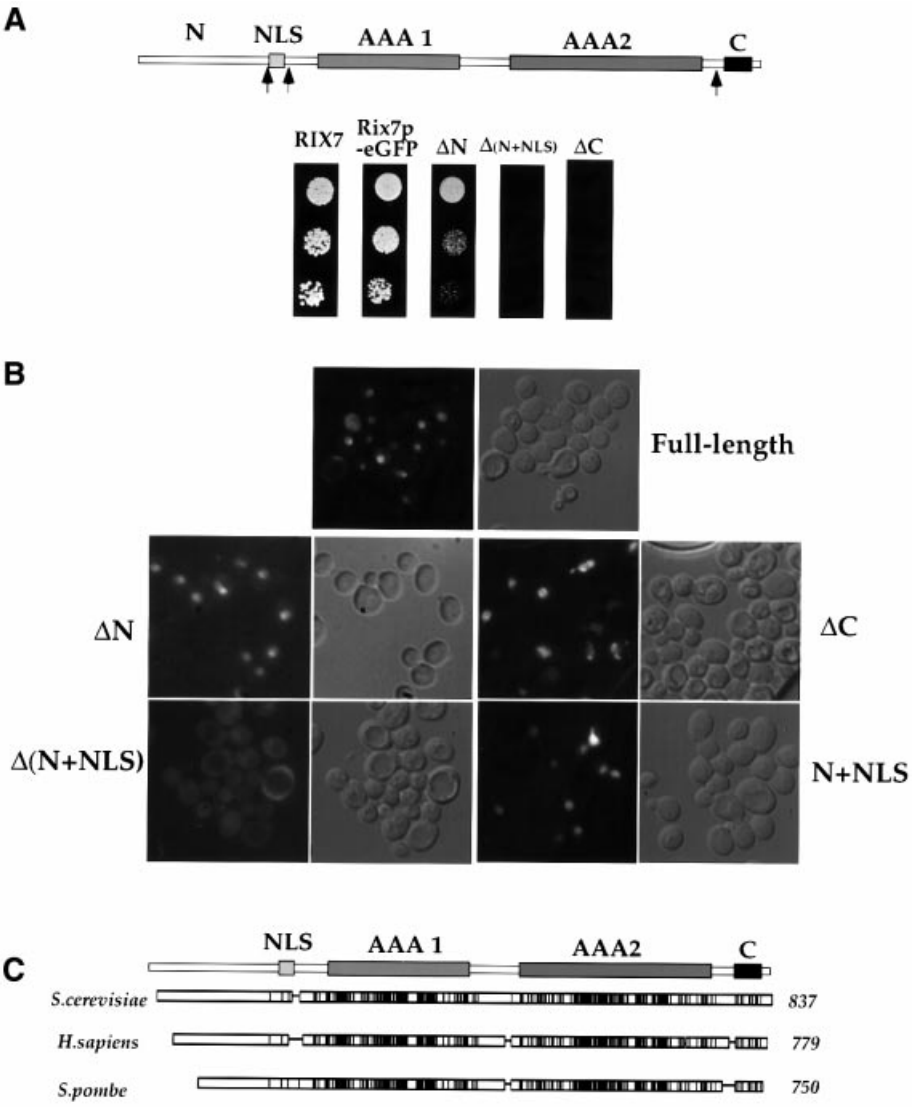

Fig. 3. Domain organization of Rix7p. (**A**) Upper panel: schematic presentation of the Rix7p sequence consisting of an N-domain (N), an NLS (residues 175–195), two consecutive AAA domains (residues 241–430 and 569–737) and a short C-terminal domain (residues 789–824). Arrows indicate the position of N- or C-terminal deletions. Lower panel: functional analysis of the Rix7p deletion constructs ΔN, Δ(N+NLS) and ΔC. The complementing activity of Rix7p–GFP, ΔN, ΔN+NLS and ΔC was tested in a *RIX7* shuffle strain by plating cells on 5-FOA-containing plates (4 days at 23°C). (**B**) Intracellular location of Rix7p–GFP and the derived N- and C-terminal deletions. Strains expressing either Rix7p–eGFP or the deletion constructs ΔN, Δ(N+NLS), ΔC and N+NLS were analysed at 23°C during the exponential growth phase by fluorescence microscopy and Nomarski imaging. (**C**) Schematic presentation of the conserved amino acids within Rix7p homologues. Black or grey rectangles denote identical and homologous residues, respectively. NCB.GenPep accession Nos: *S.cerevisiae* Rix7p (S64785), and *S.pombe* (T39584) and *Homo sapiens* (U68140) homologues.

with that in 35S processing. Some reduction in the amount of 18S rRNA was seen, probably due to the reduced growth rate of the mutant. Synthesis of tRNAs and of the 5S rRNA continued in the *rix7-1* strain, with a reduction in accumulation consistent with the reduced growth.

Together, these data indicate that strains defective in Rix7p are not primarily defective in pre-rRNA cleavage, but rapidly degrade the 27SB, and possibly 7S, pre-rRNA. This suggests that Rix7p is involved in a structural rearrangement required for correct assembly, and therefore stability, of the 60S ribosomal subunit. The kinetic delay in processing of the early sites on the pathway of 18S rRNA is probably indirect, since this has been seen for many other mutants defective in 60S synthesis (Kressler *et al*., 1999; Venema and Tollervey, 1999).

Rix7p associates with pre-ribosomes

The observed defects in 60S ribosomal biogenesis suggest that Rix7p functionally interacts with pre-ribosomes inside the nucleus. Three major ribosomal precursor particles are reported from yeast (Trapman *et al*., 1975). An early 90S particle, which contains the 35S pre-rRNA associated with many early assembling ribosomal proteins, is subsequently cleaved into 66S and 43S pre-ribosomes, the precursors to the mature 60S and 40S subunits, respectively. The 66S pre-ribosomal particle contains the 27S and 7S pre-rRNA species, whereas the 43S particle contains the 20S pre-rRNA. Protein complexes associated with the pre-ribosomal particles, the Noc1p–Noc2p and Noc2p–Noc3p complexes, have been shown to co-fractionate with the 35S and the 27S/7S pre-rRNA, respectively,

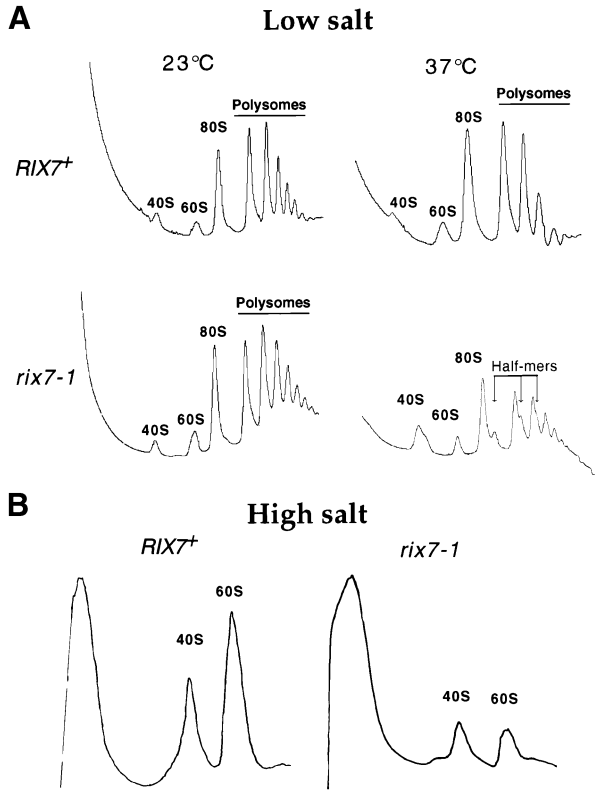

Fig. 4. *rix7-1* is impaired in 60S subunit biogenesis. Polysomal profiles ($OD_{260\ nm}$) after sucrose density gradient centrifugation derived from the *rix7-1* mutant and wild-type strain grown at permissive temperature (23°C) and 4 h after shift to restrictive temperature (37°C) under low salt (100 mM KCl) (**A**) and high salt (0.8 M KCl) conditions (**B**). The positions of 40S, 60S and 80S ribosomal particles, polysomes and 'half-mers' are indicated.

under the extraction conditions used here (Milkereit *et al*., 2001).

The association of protein A (ProtA)-tagged Rix7p with pre-ribosomal particles was assessed by sucrose gradient centrifugation and western blotting (Figure 7). The ribosomal protein Rpl10p served as a marker for 60S subunits, 80S ribosomes, and polysomes, and the Noc3p protein as a marker for 66S pre-ribosomes (see also Milkereit *et al*., 2001). When whole-cell lysates were prepared under low salt conditions, most Rix7p was found on the top of the sucrose gradient. However, a pool of Rix7p–ProtA is also seen in denser fractions of the sucrose gradient, with a peak in a zone where 60S subunits are found (Figure 7A). A more careful analysis of the fractions around 60S subunits revealed that Rix7p–ProtA co-peaks with 60S subunits, but also tails into deeper fractions of the gradient, in which pre-ribosomal particles such as 66S and 90S particles can be found (Figure 7B). In contrast, when the yeast cell extract was treated with high salt prior to centrifugation, the pool of Rix7p–ProtA peaking around 60S subunits disappeared, but 60S and 40S subunits were readily detectable (data not shown). We conclude that under steady-state conditions, a fraction of Rix7p is associated with intranuclear precursor particles to 60S large subunits. Rix7p is strongly predicted to be an enzyme and we expect only transient interactions with the pre-ribosomal particles.

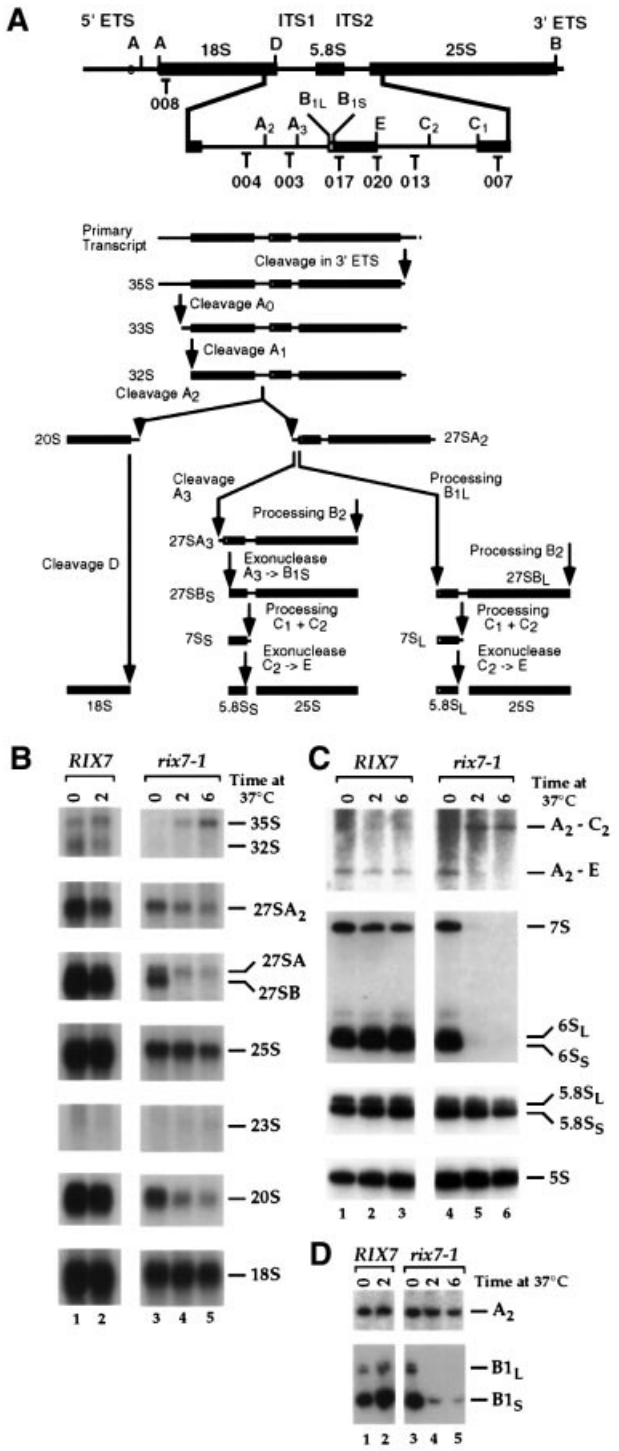

Fig. 5. Northern analysis of pre-rRNA processing in *rix7-1* cells. (**A**) Schematic diagram of the pre-rRNA processing pathway. The 35S pre-rRNA precursor contains the sequences for the mature 18S, 5.8S and 25S rRNAs separated by the two internal transcripted spacers, and flanked by the 5′-ETS and 3′-ETS. The locations of the known processing sites and rRNA precursor molecules are indicated. (**B**) Wild type (lanes 1 and 2) and *rix7-1* (lanes 3–5) were analysed following growth at 25°C (0 h samples), and 2 and 6 h after transfer to 37°C. Pre-rRNA species of high molecular weight were detected as indicated, as are the oligonucleotides used. (**C**) Pre-rRNA species of low molecular weight from wild type (lanes 1–3) and *rix7-1* (lanes 4–6) were analysed in the same way. (**D**) Primer extension analysis of wild-type (lanes 1 and 2) and *rix7-1* (lanes 3–5) cells.

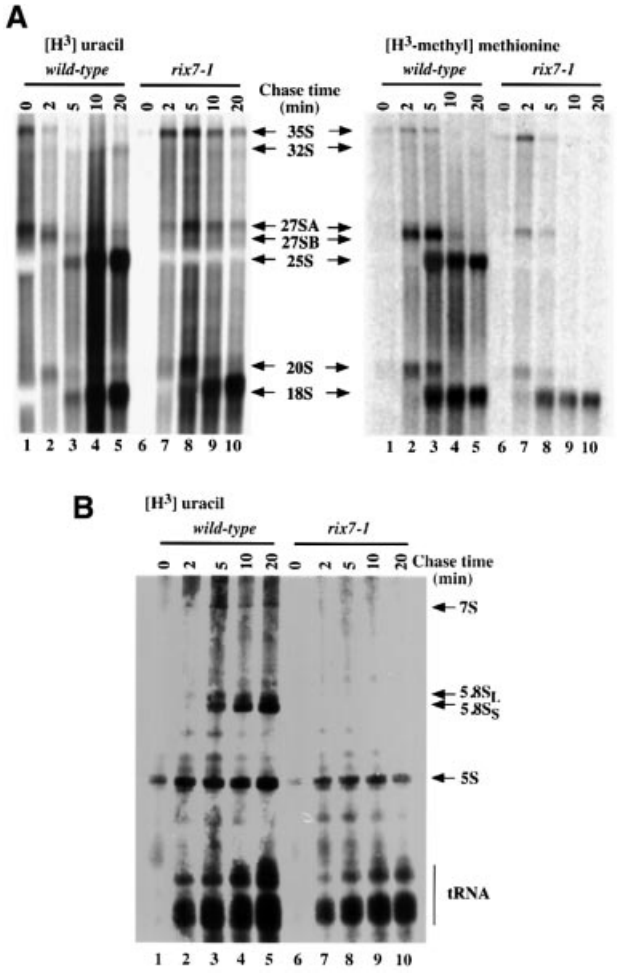

Fig. 6. Pulse–chase analysis of pre-rRNA processing in the *rix7-1* strain. Wild-type (lanes 1 –5) and *rix7-1* (lanes 6–10) strains were labelled with [^{3}H]uracil for 1 min or with [^{3}H]methyl methionine for 2 min, and then chased with unlabelled uracil or methionine for the times indicated. (**A**) High molecular weight RNA species. (**B**) Low molecular weight RNA species.

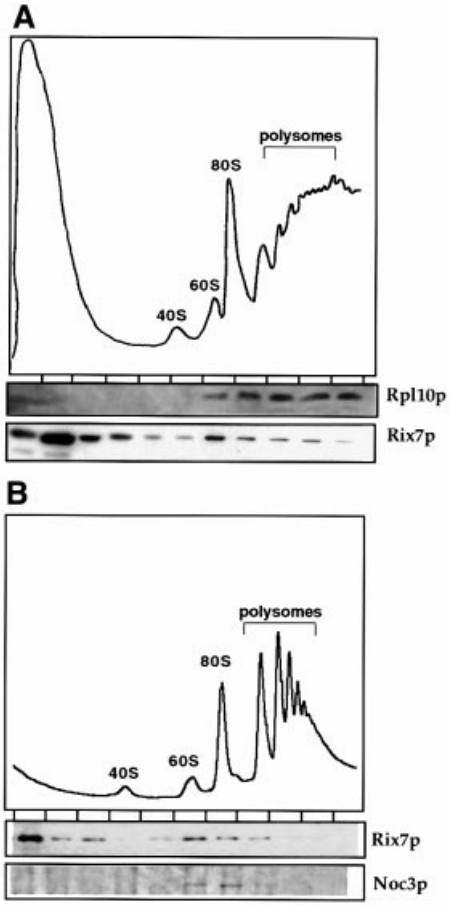

Fig. 7. A pool of Rix7p co-fractionates with pre-ribosomal particles to 60S large subunits. (**A**) Analysis of polysomal ribosome fractions derived from cells expressing Rix7p–ProtA. Fractions were analysed by SDS–PAGE and western blotting using α-Rpl10p and α-ProtA antibodies, respectively. (**B**) Comparison of Rix7p–ProtA and the 66S pre-ribosomal subunit marker Noc3p (Milkereit *et al*., 2001) on sucrose gradients. Fractions were analysed by SDS–PAGE and western blotting using α-Noc3p and α-ProtA antibodies, respectively.

Rix7p changes its intranuclear distribution depending on the growth condition

As shown above, Rix7p tagged with GFP and expressed from an *ARS/CEN* plasmid exhibits a generalized nuclear localization with no clear sub-nuclear concentration (see Figure 3B). We expressed Rix7p–GFP as a construct integrated at the *RIX7* gene locus to avoid overexpression. When cells were grown to stationary phase (OD_{600} between 5 and 10), the Rix7p–GFP signal became weaker, but was concentrated in a distinct nuclear region, apparently corresponding to the nucleolus (Figure 8A, stationary; see below). When cells in stationary phase were transferred to fresh medium for 2 h, the Rix7p–GFP signal increased and exhibited a transient perinuclear location (Figure 8A, re-induction). After prolonged growth in fresh medium, Rix7p–GFP finally regained an overall nuclear distribution (Figure 8A, exponential). As a control we used a bona fide nucleolar protein tagged with GFP, Noc1p–GFP (Milkereit *et al*., 2001), which is found in a similar distinct nuclear spot (i.e. the nucleolus) in starved cells, but remains nucleolar and does not exhibit a perinuclear location upon re-induction of growth (Figure 8A, re-induction).

This change in the intranuclear localization of Rix7p points to a dynamic localization under different growth conditions. This was also followed by time-lapse fluorescence microscopy. Similar to the above observations, Rix7p–GFP was concentrated in a distinct area of the nucleus in starved cells (Figure 8B, 0.5 h). After re-induction of growth through transfer to fresh medium (Figure 8B, 3.5 h), the nucleolar concentration of Rix7p–GFP changed to a distribution throughout the entire nucleoplasm (Figure 8B, 3.5 and 8 h). No specific changes in the pattern of Rix7p–GFP distribution were seen during mitosis.

To show that Rix7p–GFP concentrates in the nucleolus at stationary phase, it was co-expressed with the nucleolar marker DsRed–Nop1p (Gadal *et al*., 2001). The green fluorescent signal of Rix7p–GFP and the red fluorescent signal of DsRed–Nop1p largely overlapped in starved cells (Figure 8C, stationary), indicating that Rix7p–GFP indeed concentrates in the nucleolus. The peripheral nuclear location of Rix7p–GFP seen after re-induction of growth is not due to an extended nucleolus. Under these conditions,

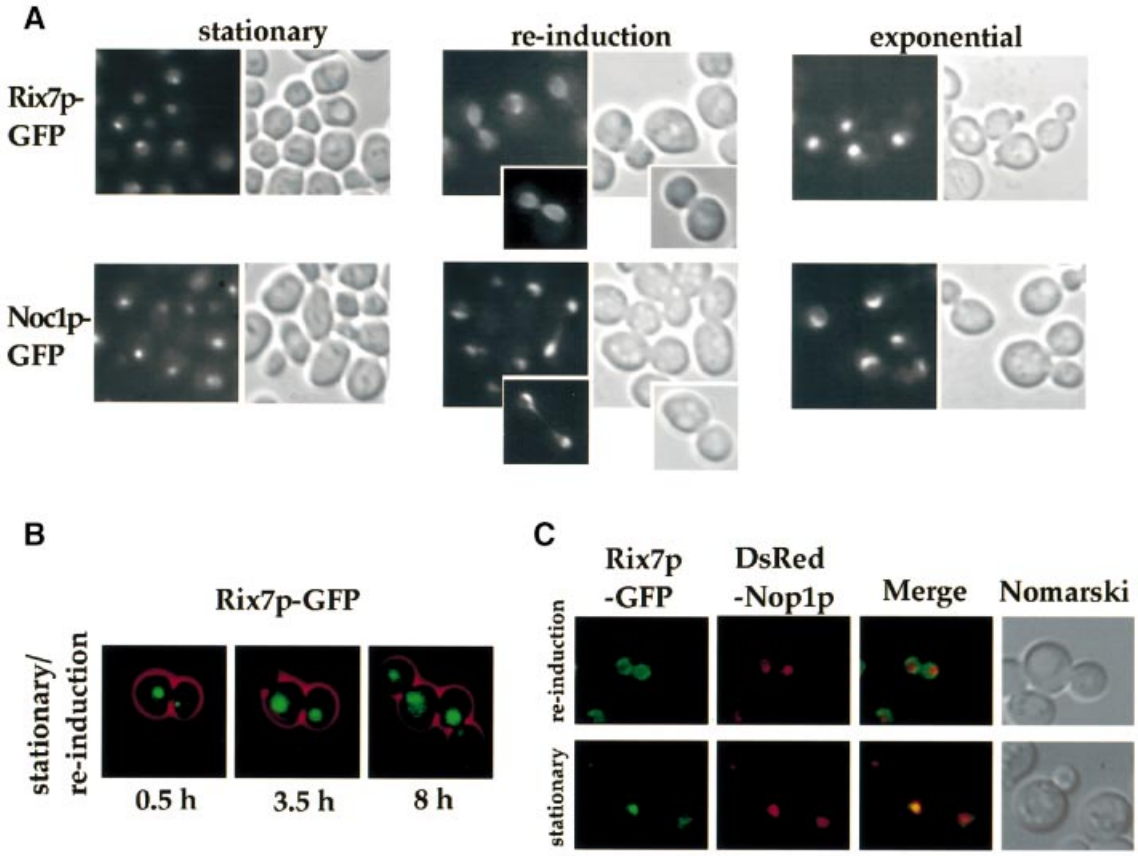

Fig. 8. Location of Rix7p–GFP in living cells grown under different growth conditions. (**A**) The Rix7–GFP (genomic integration) strain was grown at 23°C to stationary phase (OD_{600} = 5), growth re-induced in fresh YPD medium for 3 h at 23°C, and cells grown further to exponential phase (OD_{600} = 0.5). The GFP signal was monitored by fluorescence microscopy. Cells were also visualized by Nomarski imaging. The nucleolar protein Noc1p–GFP (Milkereit *et al*., 2001), which does not exhibit a transient perinuclear location during growth induction, served as a control. (**B**) Time-lapse microscopy of Rix7p–GFP from stationary cells and after re-induction in fresh YPD medium. (**C**) Rix7–GFP cells also expressing DsRed–Nop1p (pUN100-DsRed-NOP1) were analysed by fluorescence microscopy under stationary phase conditions and after growth in fresh YPD medium. The Rix7p–GFP and DsRed–Nop1p images were merged to detect co-localization.

the nucleolus remains distinct and small, and does not overlap significantly with the Rix7p–GFP signal (Figure 8C, re-induction).

We conclude from these studies that Rix7p can shuttle between the nucleolus, nucleoplasm and nuclear periphery. Alterations in the distribution of Rix7p may correlate with changes in ribosome biogenesis and transport in response to nutrient availability.

Discussion

Here, we report that a member of the superfamily of AAA ATPases (Rix7p) associates with precursor particles to 60S ribosomal subunits, and plays a role in large subunit assembly and subsequent export to the cytoplasm.

While many members of the 'DEAD-box' family of ATPases (helicases) have been implicated in ribosome assembly, this is the first report of a role for an AAA-type ATPase in ribosome biogenesis. AAA proteins are found in eukaryotes, prokaryotes and Archaea, and each organism has many different AAA proteins, which function in diverse cellular processes. The genome of *S.cerevisiae* encodes ~50 different AAA ATPases. The unifying feature of the AAA superfamily is an ATPase domain of 220 amino acids, whose structural fold has been solved recently (for reviews see Vale, 2000; Zhang *et al*., 2000). While the biological functions of the various members of this superfamily seem unrelated, a common mechanism is emerging from structural studies. AAA proteins assemble into oligomers, in most cases forming hexameric rings. A nucleotide-dependent conformational switch applies tension to bound substrates, allowing AAA proteins to unfold or dissociate attached proteins (Vale, 2000). We have no direct evidence for the oligomerization of Rix7p, but *rix7-1* exhibits a semi-dominant phenotype consistent with the incorporation of both intact and mutated subunits into an oligomeric complex. Similar observations have been made for NSF, ClpA and regulatory subunits of the proteasome (Vale, 2000).

It seems reasonable to assume that activities that can disassemble protein complexes will be required during the various stages of ribosome synthesis and during transport of pre-ribosomes from the nucleolus to the cytoplasm. A vast number of *trans*-acting factors participate in ribosome synthesis. More than 50 protein factors and >100 snoRNAs are predicted to associate with and subsequently dissociate from each pre-rRNA molecule during its intranuclear lifespan. Moreover, pre-rRNA processing in yeast is very fast, implying a rapid binding and release of many factors. This presumably entails a considerable free

Table I. Yeast strains

Name	Genotype	Origin
RS453a	MAT**a**, *ade2, leu2, ura3, his3, trp1*	Hurt *et al*. (1999)
FY23	MAT**a**, *ura3, trp1, leu2*	derived from S288C
FY86	MAT**a**, *ura3, his3, leu2*	derived from S288C
rix7-1 original	MAT**a**, *ura3, his3, leu2, rix7-1*	isolated from ts collection (Amberg *et al*., 1992)
rix7-1 a	*MAT***a**, *ura3, his3, leu2, trp1, rix7-1*	offspring of *rix7-1* original × FY86
rix7-1 α	MATα, *ura3, his3, leu2, trp1, rix7-1*	offspring of *rix7-1* original × FY86
RIX7 Shuffle	MAT**a**, *leu2*, *ura3*, *his3*, *met15*, *lys2*, rix7::KANMX4 +*pRS316-RIX7(ARS/CEN, RPL25, URA3)*	derived from Euroscarf strain Y21522
DEHQ1-1	MATα, *ade2*, *his3*, *trp1*, *leu2*, *ura3*, *can1*, qsr1Δ1::HIS3 +pHFF22 (*ARS/CEN, URA3, QSR1*)	Eisinger *et al*. (1997)
RPL10Δ *rix7-1*	MATα, *ade2*, *his3*, *trp1*, *leu2*, *ura3*, qsr1Δ1::HIS3, *rix7-1* +pHFF22 (*ARS/CEN, URA3, QSR1*)	offspring of *rix7-1 a* × DEHQ1-1
RIX7–eGFP	MATα, *leu2*, *ura3*, *his3*, *met15*, *lys2*, rix7::KANMX4 +*pRS315-RIX7-eGFP(ARS/CEN, LEU2, Rix7-eGFP)*	derived from RIX7 Shuffle
RIX7–GFP	*MAT***a**, *ura3, trp1, his3, leu2, RIX7-GFP::KANMX4*	offspring of FY23 × FY86
RIX7–ProtA	*MAT***a**, *ura3, trp1, his3, leu2, RIX7-ProtA::TRP1*	offspring of FY23 × FY86

energy change and is, therefore, likely to require a substantial input of energy. This need may, in part, be met by ATP hydrolysis, and Rix7p could be required for these steps. Growing yeast cells have enough copies of the U3 snoRNP to support ribosome synthesis for only ~1 min in the absence of recycling (at 2000 ribosomes/min), and other pre-rRNA processing factors appear to have roughly comparable abundances, underlining the potential importance of such an activity.

The very large Balbiani ring pre-mRNAs have been extensively studied in *Chironomus tentans*. For these, substantial structural rearrangement can be seen to precede nuclear export, accompanied by the loss of some but not all hnRNP proteins (Sun *et al*., 1998). It appears very probable that the export of ribosomal subunits will involve energy-dependent structural rearrangements. Close homologues of Rix7p exist in eukaryotes, but not in Archaea and bacteria, suggesting a function in ribosome synthesis that is conserved only among eukaryotes. Preparation of the ribosome subunits for nuclear transport could be such an activity. We have reported previously that a late structural rearrangement appears to convert salt-labile pre-60S particles to the mature subunits (Tollervey *et al*., 1993). Rix7p would be an obvious candidate to participate in this rearrangement.

The pre-rRNA processing phenotype observed in the *rix7-1* mutant strain is typical of defects seen in many other mutants that are defective in 60S subunit biogenesis. In almost all cases, the early pre-rRNA cleavages at sites A_0–A_2 show at least some inhibition, even when there is no clear or direct relationship between the mutant product and these cleavages (see also Milkereit *et al*., 2001; reviewed in Kressler *et al*., 1999; Venema and Tollervey, 1999). Recycling of processing and assembly factors may be inhibited in *rix7-1* cells by either a direct defect in disassembly or the nucleoplasmic accumulation of inappropriately structured 60S ribosome precursors. In either case, depletion of the pool of free factors available is envisaged to inhibit the assembly and processing of newly synthesized pre-rRNAs.

In summary, we have shown that a conserved member of the AAA-type ATPase superfamily, Rix7p, is involved in 60S subunit biogenesis. Rix7p is associated with precursor particles of the 60S subunits and apparently accompanies them from the nucleolus to the nucleoplasm. Our data suggest a model in which Rix7p acts to restructure the 60S subunits within the nucleus prior to their transport through the NPCs. In the absence of this restructuring, the subunits may not be competent for export, and are retained and rapidly degraded in the nucleus. The lack of Rix7p activity may also slow recycling of other processing factors, potentially explaining the delay in the early pre-rRNA processing steps seen in the mutant strains.

Materials and methods

Yeast strains, DNA recombinant work, and microbiological techniques

Yeast strains used in this study are listed in Table I. Microbiological techniques, plasmid transformation and recovery, mating, sporulation of diploids and tetrad analysis were carried out essentially as described (Santos-Rosa *et al*., 1998). DNA recombinant work was performed according to Maniatis *et al*. (1982).

Plasmid constructions

Plasmids pUN100-DsRed-Nop1, pRS316-Rpl25-eGFP, pNOPPA1L, pNOPGFP1L and pFA6a-GFP(S65T)-KANMX6 were described previously (Hellmuth *et al*., 1998; Longtine *et al*., 1998; Gadal *et al*., 2001). pFA6a-(2*ProtA-TEV)-TRP1 was derived from pFA6a-GFP(S65T)-TRP1 by cloning a PCR-generated fragment coding for 2×ProtA-TEV from pNOPPA1L in place of the GFP coding sequence.

RIX7 including its 5′-UTR was amplified by PCR from yeast genomic DNA. The derived fragment was cut with *Sac*I–*Bam*HI and fused in-frame to the eGFP variant present in pRS315-*RPL25*-eGFP, generating pRS315-*RIX7*-eGFP. The pRS315-*rix7-1*-eGFP plasmid was constructed in the same way, but using yeast genomic DNA extracted from the *rix7-1* strain.

Three PCR-generated fragments containing the 5′-UTR of *RIX7* and different C-terminal deletions of the *RIX7* coding sequence were generated from yeast genomic DNA: N (corresponding to residues 1–174), N+NLS (corresponding to residues 1–202) and ΔC (corresponding to residues 1–776). These three PCR-generated fragments were cut with *Sac*I–*Bam*HI and fused in-frame to the eGFP variant present in pRS315-RPL25-eGFP. N-terminal deletions of *RIX7* were amplified in two steps. The *RIX7* 5′-UTR was amplified by PCR from yeast genomic DNA, generating an *Nde*I site at the ATG codon of *RIX7*. This fragment was then cloned as a *Sac*I–*Bam*HI fragment into pRS315-RPL25-eGFP to generate pRS315-*RIX7::*eGFP. Two fragments corresponding to the

C-terminal part of *RIX7* coding sequence were generated by PCR: ΔN (residues 174–837) and ΔN+NLS (residues 202–837). These fragments were cut with *Nde*I–*Bam*HI and cloned into pRS315- *RIX7::*eGFP. These deletion constructs were expressed under the control of the *RIX7* promoter using the ATG start codon at the *Nde*I site.

Strain constructions

Genomic integration of GFP in-frame with *RIX7* was obtained as described previously (Longtine *et al*., 1998). Genomic integration of ProtA was carried out in the same way, but using the pFA6a-(2*ProtA-TEV)-TRP1 vector.

Cloning of RIX7/YLL034c

A yeast genomic library in a *LEU2*-containing *ARS/CEN* plasmid (Gautier *et al*., 1997) was transformed into the *rix7-1* strain. From colonies growing at the restrictive temperature (37°C) was isolated plasmid pRIX7 with a genomic insert. The complementing plasmid contained the *YLL034c* gene. p*YLL034c* harbouring only the *RIX7* gene was cloned and shown to complement the ts growth defect of the *rix7-1* mutant. pRS316-*RIX7* was generated by subcloning of *YLL034c* into pRS316.

Pulse–chase and northern analysis of rRNA

Pulse–chase labelling of rRNA and analysis of rRNA processing by northern hybridization were performed as described (Tollervey, 1987; Tollervey *et al*., 1993).

Oligonucleotides used were: 003: TGTTACCTCTGGGCCC; 004: CGGTTTTAATTGTCCTA; 007: CTCCGCTTATTGATATGC; 008: CATGGCTTAATCTTTGAGAC; 013: GGCCAGCAATTTCAAGTTA; 017: GCGTTGTTCATCGATGC; 020: TGAGAAGGAAATGACGCT; 219: GAAGCGCCATCTAGATG; 5′ A_0L: GGTCTCTCTGCTGCCGG.

Fluorescence microscopy

pRS315-RPL25-eGFP or pRS316-RPL25-eGFP was introduced into yeast cells by transformation, and selected on SDC-leu medium or SDC-ura medium, respectively. Individual transformants were grown in liquid SDC-leu medium at 23°C to an $OD_{600\ nm}$ of ~1, before shift to 37°C in liquid YPD medium. After centrifugation, cells were resuspended in water, mounted on a slide and viewed in the fluorescence microscope. *In vivo*, the GFP signal was examined in the fluorescent channel; the DsRed used in fusion with Nop1p was examined in the rhodamine channel of a Zeiss Axioskop fluorescence microscope and pictures were obtained with a Xillix Microimager CCD camera. Digital pictures were processed by the software program Improvision (Open lab) and Photoshop 4.0.1 (Adobe).

Time-lapse microscopy

Time-lapse microscopy was performed using the RIX7–GFP strain. Exponential growing cells (interval: 120 s; exposure: 0.2 s; transmission: 25%; Z-Planes: 3; Optovar: 1×; objective: 100× 1.3 PH3 oil) or stationary culture (interval: 180 s; exposure: 0.3 s; transmission: 50%; Z-Planes: 3; Optovar: 1×; objective: 100× 1.3 PH3 oil) were followed by confocal microscopy.

Miscellaneous

The search for functional domains was performed using the pfscan package (www.isrec.isb-sib.ch/software/PFSCAN). SDS–PAGE and western blot analysis were performed according to Siniossoglou *et al*. (1996), and isolation of ribosomes under low and high salt conditions by sucrose gradient centrifugation as described in Tollervey *et al*. (1993). Whole-cell lysates and fractions from the sucrose gradient were separated by SDS–PAGE and analysed by western blotting using the indicated antibodies. Polyclonal antiserum against Rpl10p was a kind gift of Dr Trumpower (Hanover, NH). Affinity-purified α-Noc3p antibodies were kindly obtained from Dr Tschochner (BZH, Heidelberg, Germany).

Acknowledgements

We are grateful to Dr Trumpower for providing antibodies against ribosomal proteins. We thank Dr K.Sträßer for critical reading of the manuscript. E.H. was a recipient of grants from the Deutsche Forschungsgemeinschaft (Schwerpunktprogramm 'Funktionelle Architektur des Zellkerns'), E.P. and D.T. are funded by the Wellcome Trust, and O.G. is a holder of a HFSP fellowship.

References

Amberg,D.C., Goldstein,A.L. and Cole,C.N. (1992) Isolation and characterization of *RAT1*: an essential gene of *Saccharomyces cerevisiae* required for the efficient nucleocytoplasmic trafficking of mRNA. *Genes Dev.*, **6**, 1173–1189.

Dechampesme,A.M., Koroleva,O., Leger-Silvestre,I., Gas,N. and Camier,S. (1999) Assembly of 5S ribosomal RNA is required at a specific step of the pre-rRNA processing pathway. *J. Cell Biol.*, **145**, 1369–1380.

Doye,V. and Hurt,E.C. (1997) From nucleoporins to nuclear pore complexes. *Curr. Opin. Cell Biol.*, **9**, 401–411.

Eisinger,D.P., Dick,F.A. and Trumpower,B.L. (1997) Qsr1p, a 60S ribosomal subunit protein, is required for joining of 40S and 60S subunits. *Mol. Cell. Biol.*, **17**, 5136–5145.

Gadal,O., Strauβ,D., Kessl,J., Trumpower,B., Tollervey,D. and Hurt,E. (2001) Nuclear export of 60S ribosomal subunits depends on Xpo1p and requires a NES-containing factor Nmd3p that associates with the large subunit protein Rpl10p. *Mol. Cell. Biol.*, **21**, 3405–3415.

Gautier,T., Bergès,T., Tollervey,D. and Hurt,E. (1997) Nucleolar KKE/D repeat proteins Nop56p and Nop58p interact with Nop1p and are required for ribosome biogenesis. *Mol. Cell. Biol.*, **17**, 7088–7098.

Germain-Lee,E.L., Obie.,C. and Valle,D. (1997) NVL: a new member of the AAA family of ATPases localized to the nucleus. *Genomics*, **44**, 22–34.

Hellmuth,K., Lau,D.M., Bischoff,F.R., Künzler,M., Hurt,E.C. and Simos,G. (1998) Yeast Los1p has properties of an exportin-like nucleocytoplasmic transport factor for tRNA. *Mol. Cell. Biol.*, **18**, 6374–6386.

Ho,J.H., Kallstrom,G. and Johnson,A.W. (2000) Nmd3p is a Crm1p-dependent adapter protein for nuclear export of the large ribosomal subunit. *J. Cell Biol.*, **151**, 1057–1066.

Hurt,E., Hannus,S., Schmelzl,B., Lau,D., Tollervey,D. and Simos,G. (1999) A novel *in vivo* assay reveals inhibition of ribosomal nuclear export in Ran-cycle and nucleoporin mutants. *J. Cell Biol.*, **144**, 389–401.

Kadowaki,T., Zhao,Y. and Tartakoff,A.M. (1992) A conditional yeast mutant deficient in mRNA transport from nucleus to cytoplasm. *Proc. Natl Acad. Sci. USA*, **89**, 2312–2316.

Kressler,D., Linder,P. and De La Cruz,J. (1999) Protein *trans*-acting factors involved in ribosome biogenesis in *Saccharomyces cerevisiae*. *Mol. Cell. Biol.*, **19**, 7897–7912.

Longtine,M.S., McKenzie,A., Demarini,D.J., Shah,N.G., Wach,A., Brachat,A., Philippsen,P. and Pringle,J.R. (1998) Additional modules for versatile and economical PCR-based gene deletion and modification in *Saccharomyces cerevisiae*. *Yeast*, **14**, 953–961.

Maniatis,T., Fritsch,E.T. and Sambrook,J. (1982) *Molecular Cloning: A Laboratory Manual.* Cold Spring Harbor Laboratory Press, Cold Spring Harbor, NY.

Milkereit,P. *et al*. (2001) Maturation and intranuclear transport of pre-ribosomes requires Noc proteins. *Cell*, **105**, 499–509.

Neuwald,A.F., Aravind,L., Spouge,J.L. and Koonin,E.V. (1999) AAA+: a class of chaperone-like ATPases associated with the assembly, operation, and dissassembly of proteins complexes. *Genome Res.*, **9**, 27–43.

Rouiller,I., Butel,V.M., Latterich,M., Milligan,R.A. and Wilson-Kubalek, E.M. (2000) A major conformational change in p97 AAA ATPase upon ATP binding. *Mol. Cell*, **6**, 1485–1490.

Rout,M.P., Aitchison,J.D., Suprapto,A., Hjertaas,K., Zhao,Y. and Chait,B.T. (2000). The yeast nuclear pore complex: composition, architecture and transport mechanism. *J. Cell Biol.*, **148**, 635–651.

Santos-Rosa,H., Moreno,H., Simos,G., Segref,A., Fahrenkrog,B., Panté,N. and Hurt,E. (1998) Nuclear mRNA export requires complex formation between Mex67p and Mtr2p at the nuclear pores. *Mol. Cell. Biol.*, **18**, 6826–6838.

Sarkar,S., Azad,A.K. and Hopper,A.K. (1999) Nuclear tRNA aminoacylation and its role in nuclear export of endogenous tRNAs in *Saccharomyces cerevisiae*. *Proc. Natl Acad. Sci. USA*, **96**, 14366–14371.

Segref,A., Sharma,K., Doye,V., Hellwig,A., Huber,J., Lührmann,R. and Hurt,E.C. (1997) Mex67p which is an essential factor for nuclear mRNA export binds to both poly(A)$^+$ RNA and nuclear pores. *EMBO J.*, **16**, 3256–3271.

Siniossoglou,S., Wimmer,C., Rieger,M., Doye,V., Tekotte,H., Weise,C., Emig,S., Segref,A. and Hurt,E.C. (1996) A novel complex of nucleoporins, which includes Sec13p and a Sec13p homolog, is essential for normal nuclear pores. *Cell*, **84**, 265–275.

Stade,K., Ford,C.S., Guthrie,C. and Weis,K. (1997) Exportin 1 (Crm1p) is an essential nuclear export factor. *Cell*, **90**, 1041–1050.

Stage-Zimmermann,T., Schmidt,U. and Silver,P.A. (2000) Factors affecting nucler export of the 60S subunits *in vivo*. *Mol. Biol. Cell*, **11**, 3777–3789.

Sun,X., Alzhanova-Ericsson,A.T., Visa,N., Aissouni,Y., Zhao,J. and Daneholt,B. (1998) The hrp23 protein in the Balbiani ring pre-mRNP particles is released just before or at the binding of the particles to the nuclear pore complex. *J. Cell Biol.*, **142**, 1181–1193.

Tollervey,D. (1987) A yeast small nuclear RNA is required for normal processing of pre-ribosomal RNA. *EMBO J.*, **6**, 4169–4175.

Tollervey,D., Lehtonen,H., Jansen,R.P., Kern,H. and Hurt,E.C. (1993) Temperature-sensitive mutations demonstrate roles for yeast fibrillarin in pre-rRNA processing, pre-rRNA methylation and ribosome assembly. *Cell*, **72**, 443–457.

Trapman,J., Retel,J. and Planta,R.J. (1975) Ribosomal precursor particles from yeast. *Exp. Cell Res.*, **90**, 95–104.

Vale,R.D. (2000) AAA proteins: lords of the ring. *J. Cell Biol.*, **150**, 13–19.

Van Beekvelt,C.A., Kooi,E.A., de Graaff-Vincent,M., Riet J., Venema,J. and Raue,H.A. (2000) Domain III of *Saccharomyces cerevisiae* 25 S ribosomal RNA: its role in binding of ribosomal protein L25 and 60 S subunit formation. *J. Mol. Biol.*, **296**, 7–17.

Venema,J. and Tollervey,D. (1999) Ribosome synthesis in *Saccharomyces cerevisiae*. *Annu. Rev. Genet.*, **33**, 261–311.

Woolford,J.L.,Jr (1991) The structure and biogenesis of yeast ribosomes. *Adv. Genet.*, **29**, 63–118.

Zhang,X. *et al*. (2000) Structure of the AAA ATPase p97. *Mol. Cell*, **6**, 1473–1484.

Received March 13, 2001; revised May 25, 2001;
accepted May 29, 2001